Proceedings of DETC'03
ASME 2003 Design Engineering Technical Conferences and
Computers and Information in Engineering Conference
Chicago, Illinois, USA, September 2-6, 2003

DETC2003/VIB-48603

MODAL INTERACTIONS IN A THERMALLY LOADED ANNULAR PLATE

Haider N. Arafat*
Ali H. Nayfeh†
Department of Engineering Science and Mechanics, MC 0219
Virginia Polytechnic Institute and State University
Blacksburg, Virginia 24061, U.S.A.
(540) 231-5453/Fax: (540) 231-2290/anayfeh@vt.edu

ABSTRACT

We investigate the nonlinear forced vibrations of a thermally loaded annular plate with clamped-clamped immovable boundary conditions in the presence of a three-to-one internal resonance between the first and second axisymmetric modes. We consider the in-plane thermal load to be axisymmetric and excite the plate externally by a harmonic force near primary resonance of the second mode. We then use the nonlinear von Kármán plate equations to model the behavior of the system and apply the method of multiple scales to investigate its responses. We found that the response can be periodic oscillations consisting of both modes, with a large component from the first mode. Moreover, the periodic solutions may undergo Hopf bifurcations which lead to aperiodic oscillations of the plate.

Keywords: *Annular plates, thermal load, three-to-one internal resonance, modal interactions, nonlinear vibrations.*

INTRODUCTION

The influence of modal interactions in systems is of great interest to engineers because they can lead to unexpected and unwanted large and complex responses [1]. In particular, modal interactions in circular plates are important because the nature of the response can also be affected. That is, the response may consist of standing waves, traveling waves, or both.

Sridhar, Mook, and Nayfeh [2,3] considered the response of a circular plate under a primary resonance excitation $\Omega \approx \omega_{rs}$ in the presence of a combination internal resonance of the type $\omega_{ij} + 2\omega_{kl} \approx \omega_{mn}$. They considered in Ref. [2] interactions between axisymmetric modes only and in Ref. [3] interactions between axisymmetric and asymmetric modes. In the latter case, they found that a traveling-wave response may occur when $\Omega \approx \omega_{mn}$. Hadian and Nayfeh [4] analyzed a plate having the internal resonance $\omega_{01} + 2\omega_{02} \approx \omega_{03}$ and found that, when $\Omega \approx \omega_{03}$, the multimode responses found in Ref. [2] may undergo a Hopf bifurcation, resulting in a quasiperiodic multimodal motion. Moreover, this motion could develop into a chaotic one as a result of undergoing a sequence of period-doubling bifurcations. Lee and Kim [5] also considered a plate having the internal resonance $\omega_{01} + 2\omega_{02} \approx \omega_{03}$, but they excited it by the external combination resonance $\Omega \approx 2\omega_{01} + \omega_{02}$. They found interactions among the modes. Yeo and Lee [6] introduced a correction to the evolution equations derived in Ref. [3] and then considered the response due to a primary resonance of the asymmetric mode ω_{11} (i.e., $\Omega \approx \omega_{11}$). They found that, even without considering any internal resonances, the response of the plate can consist of a traveling wave for a certain range of parameters.

Plates are key components in many structural and machinery applications. Some examples include flight-vehicle power plants, tanks, brake systems in automotive vehicles, and, more recently, microelectromechanical (MEMS) devices, such as sensors and micropumps. In many of these applications, the plates are subjected to thermal loads, which may cause buckling and/or induce

*Postdoctoral Research Associate. ASME Member
†University Distinguished Professor. ASME Fellow. Address all correspondence to this author.

unexpected dynamic responses [7]. Consequently, the responses of plates to thermal loadings are the subject of much research [8,9]. Next, we review the research done on annular and circular plates in this field and separate it into linear and nonlinear analyses.

Fedorov [10] examined the linear thermostability problem of elastically clamped variable-stiffness annular plates under axisymmetric radial nonuniform thermal loads. He found that, in certain cases, variation of the Young modulus and Poisson ratio with temperature cannot be neglected. Irie and Yamada [11] investigated the linear free vibrations of elastically supported circular and annular plates, with one edge exposed to an axisymmetric sinusoidal heat flux and the other edge thermally insulated. Buckens [12] investigated the linear free pre- and post-buckling vibrations of a circular plate under in-plane thermal stresses.

Using Berger's approximation, Pal [13-15] investigated the nonlinear responses of isotropic and orthotropic circular heated plates under different thermal conditions. He compared his results with the solution of the von Kármán equations and concluded that Berger's approximation yields valid results. Biswas and Kapoor [16] used the von Kármán equations to study the nonlinear vibrations of polar orthotropic clamped circular plates at elevated temperatures. They concluded that the effect of the in-plane thermal stress is to decrease the period of oscillations. Li, Zhou, and Song [17] used the von Kármán equations to study the nonlinear free vibrations of isotropic and polar orthotropic annular plates carrying a concentric rigid mass and subject to thermal loads. They then applied the Kantorovich averaging method and examined the nonlinear natural frequencies and thermal buckling loads for hinged and clamped immovable boundary conditions. The nonlinear vibrations of a simply-supported circular plate under a thermally induced principal parametric excitation of an axisymmetric mode (i.e., $\Omega \approx 2\omega_{0k}$) was investigated by Nayfeh and Faris [18]. They [19] also investigated the nonlinear vibrations of a clamped circular plate under a thermally induced combination parametric excitation of two axisymmetric modes (i.e., $\Omega \approx \omega_{0j} + \omega_{0k}$).

In the aforementioned works on thermally loaded circular plates, the influence of internal resonances on the response was never investigated. In studying the linear free vibration problem of circular and annular plates under an axisymmetric thermal loading, as shown in Fig. 1, Arafat et al. [20] found that, as the thermal load is increased, the natural frequencies can become near-commensurate with each other, possibly giving rise to internal resonances. For example, one-to-one, three-to-one, and combination internal resonances could be activated among different axisymmetric and asymmetric modes at different levels of the thermal load.

In this work, we investigate the nonlinear forced vibrations of a thermally loaded annular plate (see Fig. 1) with clamped-clamped immovable boundary conditions in the presence of a three-to-one internal resonance between the first and second axisymmetric modes (i.e., $\omega_{02} \approx 3\omega_{01}$). We excite the plate externally by a harmonic force near primary resonance of the second mode (i.e., $\Omega \approx \omega_{02}$) and consider the in-plane thermal load to be axisymmetric. We use the nonlinear von Kármán plate equations to model the behavior of the system and apply the method of multiple scales [21] to investigate its responses.

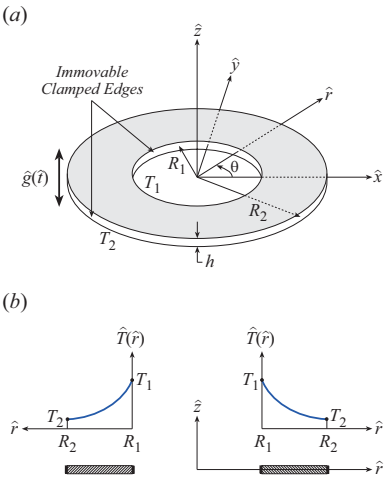

Figure 1. A schematic of (*a*) an annular plate and (*b*) a cross-sectional view illustrating a typical steady-state axisymmetric temperature distribution.

PROBLEM FORMULATION

Because the temperature distribution, external excitation, and the modes excited, either directly or indirectly, are axisymmetric, the stress function and in-plane displacements are also axisymmetric, and hence $\frac{\partial}{\partial\theta} = 0$. Accordingly, the nonlinear axisymmetric vibrations of an annular plate under an axisymmetric thermal load are governed by

$$D\hat{\nabla}^4\hat{w} + \rho h\frac{\partial^2\hat{w}}{\partial\hat{t}^2} + \hat{c}\frac{\partial\hat{w}}{\partial\hat{t}} = \frac{1}{\hat{r}}\frac{\partial^2\hat{w}}{\partial\hat{r}^2}\frac{\partial\hat{F}}{\partial\hat{r}} + \frac{1}{\hat{r}}\frac{\partial^2\hat{F}}{\partial\hat{r}^2}\frac{\partial\hat{w}}{\partial\hat{r}} - \frac{1}{(1-\nu)}\hat{\nabla}^2\hat{M}_T + \hat{g}(\hat{t}) \tag{1}$$

$$k\hat{\nabla}^2\hat{T} + \hat{Q} = \rho c_p\frac{\partial\hat{T}}{\partial\hat{t}} + \frac{E\alpha T_0}{1-2\nu}\frac{\partial e}{\partial\hat{t}} \tag{2}$$

$$\hat{g}(\hat{t}) = \hat{G}\cos(\hat{\Omega}\hat{t}) \tag{3}$$

$$\hat{M}_T = E\alpha\int_{-\frac{h}{2}}^{\frac{h}{2}}\left[\hat{T}(\hat{r},\hat{t}) - T_0\right]\hat{z}\,d\hat{z} = 0 \tag{4}$$

$$\hat{\nabla}^4 = \hat{\nabla}^2\hat{\nabla}^2 = \left(\frac{\partial^2}{\partial\hat{r}^2} + \frac{1}{\hat{r}}\frac{\partial}{\partial\hat{r}}\right)\left(\frac{\partial^2}{\partial\hat{r}^2} + \frac{1}{\hat{r}}\frac{\partial}{\partial\hat{r}}\right) \tag{5}$$

Here, $\hat{r}$ and θ are polar coordinates; $\hat{t}$ is time; $\hat{w}$ is the plate transverse displacement; $\hat{F}$ is the stress function; $\hat{u}$ and $\hat{v}$ are the radial and hoop displacements, respectively; $\hat{T}$ is the axisymmetric temperature distribution; T_0 is the initial stress-free temperature; $\hat{G}$ and $\hat{\Omega}$ are the amplitude and frequency of the external harmonic excitation $\hat{g}$; $\hat{c}$ is the damping coefficient; ρ is the material density; h is the plate thickness; e is the dilatational strain due to the thermal effect; c_p is the heat-capacity coefficient at constant pressure; α is the coefficient of thermal expansion; k is the thermal conductivity; E is the modulus of elasticity, ν is Poisson's ratio, and $D = \frac{Eh^3}{12(1-\nu^2)}$ is the bending rigidity. In this paper, we consider the case in which the heat flux $\hat{Q} = 0$.

For the compatibility relation, we note that

$$\varepsilon_r = \frac{1}{Eh}\left(\hat{N}_r - \nu\hat{N}_\theta\right) + \alpha(\hat{T} - T_0) \tag{6}$$

$$\varepsilon_\theta = \frac{1}{Eh}\left(\hat{N}_\theta - \nu\hat{N}_r\right) + \alpha(\hat{T} - T_0) \tag{7}$$

$$\hat{N}_r = \frac{1}{\hat{r}}\frac{\partial\hat{F}}{\partial\hat{r}} \quad \text{and} \quad \hat{N}_\theta = \frac{\partial^2\hat{F}}{\partial\hat{r}^2} \tag{8}$$

$$\varepsilon_r = \frac{\partial\hat{u}}{\partial\hat{r}} + \frac{1}{2}\left(\frac{\partial\hat{w}}{\partial\hat{r}}\right)^2 \quad \text{and} \quad \varepsilon_\theta = \frac{\hat{u}}{\hat{r}} \tag{9}$$

Therefore, it follows from Eqs. (6)-(9) that

$$\frac{\partial\hat{u}}{\partial\hat{r}} = -\frac{1}{2}\left(\frac{\partial\hat{w}}{\partial\hat{r}}\right)^2 + \frac{1}{Eh}\left(\frac{1}{\hat{r}}\frac{\partial\hat{F}}{\partial\hat{r}} - \nu\frac{\partial^2\hat{F}}{\partial\hat{r}^2}\right) + \alpha(\hat{T} - T_0) \tag{10}$$

$$\frac{\hat{u}}{\hat{r}} = \frac{1}{Eh}\left(\frac{\partial^2\hat{F}}{\partial\hat{r}^2} - \frac{\nu}{\hat{r}}\frac{\partial\hat{F}}{\partial\hat{r}}\right) + \alpha(\hat{T} - T_0) \tag{11}$$

Then, after eliminating $\hat{u}$ from Eqs. (10) and (11), we obtain the compatibility equation

$$\hat{r}\frac{\partial^3\hat{F}}{\partial\hat{r}^3} + \frac{\partial^2\hat{F}}{\partial\hat{r}^2} - \frac{1}{\hat{r}}\frac{\partial\hat{F}}{\partial\hat{r}} = -Eh\alpha\hat{r}\frac{\partial\hat{T}}{\partial\hat{r}} - \frac{1}{2}Eh\left(\frac{\partial\hat{w}}{\partial\hat{r}}\right)^2 \tag{12}$$

The associated boundary conditions for a clamped-clamped annular plate are as follows:

$$\hat{w} = 0 \text{ and } \frac{\partial\hat{w}}{\partial\hat{r}} = 0 \text{ at } \hat{r} = R_1, R_2 \tag{13}$$

$$\hat{T} = T_1 \text{ at } \hat{r} = R_1 \tag{14}$$

$$\hat{T} = T_2 \text{ at } \hat{r} = R_2 \tag{15}$$

where R_1 and R_2 are the inner and outer radii, respectively, and T_1 and T_2 are constant temperatures. In addition, because both of the inner and outer boundaries are assumed to be immovable, the radial deflection $\hat{u}$ must vanish at $\hat{r} = R_1$ and $\hat{r} = R_2$. Hence, it follows from Eq. (11) that

$$\frac{\partial^2\hat{F}}{\partial\hat{r}^2} - \frac{\nu}{\hat{r}}\frac{\partial\hat{F}}{\partial\hat{r}} + Eh\alpha(\hat{T} - T_0) = 0 \text{ at } \hat{r} = R_1, R_2 \tag{16}$$

SOLUTION PROCEDURE

The terms on the right-hand side of Eq. (2) represent, respectively, the diffusion of heat and thermoelastic coupling [22]. As discussed by Boley and Weiner [23], the thermoelastic coupling term is typically relevant to problems where the response is affected by heat dissipation through the body. In this case, the heat dissipation occurs at a much slower rate compared to the vibrations of the plate, and hence the effects of these terms may be neglected. Moreover, in the absence of a heat flux (i.e., $\hat{Q} = 0$), the temperature of the plate will be steady. Therefore, Eq. (2) reduces to

$$\hat{\nabla}^2\hat{T} = 0 \tag{17}$$

The solution of Eqs. (14), (15), and (17) yields the following temperature distribution over the plate:

$$\hat{T}(\hat{r}) = \frac{(T_1\ln R_2 - T_2\ln R_1) - (T_1 - T_2)\ln\hat{r}}{(\ln R_2 - \ln R_1)} \tag{18}$$

Next, we substitute Eq. (18) into Eq. (12) and obtain the equation governing the stress function $\hat{F}$ as:

$$\hat{r}\frac{\partial^3\hat{F}}{\partial\hat{r}^3} + \frac{\partial^2\hat{F}}{\partial\hat{r}^2} - \frac{1}{\hat{r}}\frac{\partial\hat{F}}{\partial\hat{r}} = Eh\alpha\Lambda - \frac{1}{2}Eh\left(\frac{\partial\hat{w}}{\partial\hat{r}}\right)^2 \tag{19}$$

where $\Lambda = \frac{T_2 - T_1}{\ln R_1 - \ln R_2}$. The solution of Eqs. (16) and (19) is

$$\hat{F}(\hat{r},\hat{t}) = \hat{C}_1\hat{r}^2 + \hat{C}_2\ln\hat{r} + \hat{C}_3 + \frac{1}{4}Eh\alpha\Lambda\hat{r}^2(\ln\hat{r} - 1) + \hat{\Phi}(\hat{r},\hat{t}) \tag{20}$$

$$\begin{aligned}\hat{C}_1 = \frac{Eh\alpha}{8(1-\nu)}\Bigg\{&\frac{4R_2^2(T_2 - T_0)}{R_1^2 - R_2^2} - \frac{4R_1^2(T_1 - T_0)}{R_1^2 - R_2^2} \\ &+ \frac{\Lambda R_2^2[1 + \nu + 2(1-\nu)\ln R_2]}{R_1^2 - R_2^2} \\ &- \frac{\Lambda R_1^2[1 + \nu + 2(1-\nu)\ln R_1]}{R_1^2 - R_2^2}\Bigg\}\end{aligned} \tag{21}$$

$$\hat{C}_2 = -\frac{1}{2}Eh\alpha\frac{R_1^2R_2^2(T_1 - T_2)}{R_1^2 - R_2^2} \tag{22}$$

The coefficient $\hat{C}_3$ is arbitrary and the function $\hat{\Phi}(\hat{r},\hat{t})$ is the solution of the boundary-value problem:

$$\hat{r}\frac{\partial^3\hat{\Phi}}{\partial\hat{r}^3}+\frac{\partial^2\hat{\Phi}}{\partial\hat{r}^2}-\frac{1}{\hat{r}}\frac{\partial\hat{\Phi}}{\partial\hat{r}}=-\frac{1}{2}Eh\left(\frac{\partial\hat{w}}{\partial\hat{r}}\right)^2 \tag{23}$$

$$\frac{\partial^2\hat{\Phi}}{\partial\hat{r}^2}-\frac{\nu}{\hat{r}}\frac{\partial\hat{\Phi}}{\partial\hat{r}}=0 \text{ at } \hat{r}=R_1,R_2 \tag{24}$$

We then substitute Eq. (20) into Eq. (1) and obtain the following equation governing the nonlinear axisymmetric vibrations of a thermally loaded annular plate:

$$D\hat{\nabla}^4\hat{w}+\frac{1}{\hat{r}}\frac{\partial}{\partial\hat{r}}\left[\hat{K}(\hat{r})\frac{\partial\hat{w}}{\partial\hat{r}}\right]+\rho h\frac{\partial^2\hat{w}}{\partial\hat{t}^2}=\frac{1}{\hat{r}}\frac{\partial^2\hat{w}}{\partial\hat{r}^2}\frac{\partial\hat{\Phi}}{\partial\hat{r}}+\frac{1}{\hat{r}}\frac{\partial^2\hat{\Phi}}{\partial\hat{r}^2}\frac{\partial\hat{w}}{\partial\hat{r}}-\hat{c}\frac{\partial\hat{w}}{\partial\hat{t}}+\hat{g}(\hat{t}) \tag{25}$$

$$\hat{K}(\hat{r})=-2\hat{C}_1\hat{r}-\frac{\hat{C}_2}{\hat{r}}-\frac{Eh\alpha\Lambda}{4}\hat{r}(2\ln\hat{r}-1) \tag{26}$$

subject to the boundary conditions in Eq. (13).

NONDIMENSIONAL PROBLEM

To better understand the problem at hand and ascertain the critical parameters influencing the response behavior, we introduce the following nondimensional variables and parameters:

$$r=\frac{\hat{r}}{R_2},\ t=\frac{1}{R_2^2}\sqrt{\frac{D}{\rho h}}\hat{t},\ \tau=\frac{T_1-T_0}{T_2-T_0},\ \Delta T=\frac{\hat{T}-T_0}{T_2-T_0},$$
$$w=\frac{R_2}{h^2}\hat{w},\ \Phi=\frac{R_2^2}{Eh^5}\hat{\Phi},\ b=\frac{R_1}{R_2},\ c=\frac{R_2^2}{\sqrt{\rho hD}}\hat{c},\ z=\frac{\hat{z}}{h},$$
$$g(t)=\frac{R_2^5}{Dh^2}\hat{g}(\hat{t}),\ G=\frac{R_2^5}{Dh^2}\hat{G},\ \Omega=R_2^2\sqrt{\frac{\rho h}{D}}\hat{\Omega} \tag{27}$$

Of particular importance are the parameters τ, the ratio of the absolute temperature at the inner radius to the absolute temperature at the outer radius, and b, the ratio of the inner radius to the outer radius of the annulus. Then, Eqs. (13) and (23)-(25) reduce to the following:

$$\nabla^4 w+p\frac{1}{r}\frac{\partial}{\partial r}\left[K(r)\frac{\partial w}{\partial r}\right]+\frac{\partial^2 w}{\partial t^2}=\varepsilon\left(\frac{1}{r}\frac{\partial^2 w}{\partial r^2}\frac{\partial\Phi}{\partial r}+\frac{1}{r}\frac{\partial^2\Phi}{\partial r^2}\frac{\partial w}{\partial r}\right)-c\frac{\partial w}{\partial t}+g(t) \tag{28}$$

$$w=0,\quad \frac{\partial w}{\partial r}=0,\quad \text{at}\quad r=b,1 \tag{29}$$

$$r\frac{\partial^3\Phi}{\partial r^3}+\frac{\partial^2\Phi}{\partial r^2}-\frac{1}{r}\frac{\partial\Phi}{\partial r}=-\frac{1}{2}\left(\frac{\partial w}{\partial r}\right)^2 \tag{30}$$

$$\frac{\partial^2\Phi}{\partial r^2}-\frac{\nu}{r}\frac{\partial\Phi}{\partial r}=0\quad \text{at}\quad r=b,1 \tag{31}$$

where the external forcing is given by $g(t)=G\cos(\Omega t)$, p is a measure of the thermal loading defined as

$$p=\frac{12(1+\nu)\alpha(T_2-T_0)R_2^2}{h^2}, \tag{32}$$

and ε is a small scaling parameter defined as

$$\varepsilon=\frac{12(1-\nu^2)h^2}{R_2^2}\ll 1 \tag{33}$$

Typical values for the parameter ε for thin metallic ($\nu=0.3$) plates having $h/R_2=1/25$, $1/50$, and $1/100$ are 0.0175, 0.0044, and 0.0011, respectively. Moreover, the spatial function $K(r)$ is given by

$$K(r)=-2C_1 r-\frac{C_2}{r}-\frac{(1-\tau)(1-\nu)}{4\ln b}r(2\ln r-1) \tag{34}$$

$$C_1=\frac{\left\{b^2\left[(1+\tau)-\nu(1-\tau)\right]-2\right\}}{4(1-b^2)}-\frac{(1+\nu)(1-\tau)}{8\ln b} \tag{35}$$

$$C_2=-\frac{b^2(1-\nu)(1-\tau)}{2(1-b^2)} \tag{36}$$

In Eq. (28), ∇^4 is given by Eq. (5) after dropping the hat "ˆ". In addition, from Eqs. (18) and (27), the nondimensional temperature distribution is given by

$$\Delta T(r)=1+(\tau-1)\frac{\ln r}{\ln b} \tag{37}$$

so that $\Delta T(b)=\tau$ and $\Delta T(1)=1$.

RESPONSE ANALYSIS

Equations (28)-(31) are a nonlinear partial-differential system with variable coefficients. Therefore, we propose to use a combination of perturbation and numerical methods to determine approximate solutions. To this end, we apply the method of multiple scales [21] to Eqs. (28)-(31) and introduce $t_0\equiv t$ and $t_1\equiv\varepsilon t$ as the fast and slow time scales. The first and second derivatives with time become

$$\frac{\partial}{\partial t}=D_0+\varepsilon D_1+\cdots \text{ and } \frac{\partial^2}{\partial t^2}=D_0^2+2\varepsilon D_0D_1+\cdots \tag{38}$$

where $D_n \equiv \frac{\partial}{\partial t_n}$. Then, we order the excitation and damping as $G \to \varepsilon G$ and $c \to \varepsilon c$, so that they balance the nonlinearities. Next, we expand the solutions in power series of ε as

$$w(r,t) = w_0(r,T_0,T_1) + \varepsilon w_1(r,T_0,T_1) + \cdots \tag{39}$$

$$\Phi(r,t) = \Phi_0(r,T_0,T_1) + \cdots \tag{40}$$

and obtain from Eqs. (28)-(31) the following hierarchy of problems:

Order 1:

$$D_0^2 w_0 + p\frac{1}{r}\frac{\partial}{\partial r}\left[K(r)\frac{\partial w_0}{\partial r}\right] + \nabla^4 w_0 = 0 \tag{41}$$

$$w_0 = 0, \quad \frac{\partial w_0}{\partial r} = 0 \quad \text{at} \quad r = b, 1 \tag{42}$$

$$r\frac{\partial^3 \Phi_0}{\partial r^3} + \frac{\partial^2 \Phi_0}{\partial r^2} - \frac{1}{r}\frac{\partial \Phi_0}{\partial r} = -\frac{1}{2}\left(\frac{\partial w_0}{\partial r}\right)^2 \tag{43}$$

$$\frac{\partial^2 \Phi_0}{\partial r^2} - \frac{\nu}{r}\frac{\partial \Phi_0}{\partial r} = 0 \quad \text{at} \quad r = b, 1 \tag{44}$$

Order ε:

$$D_0^2 w_1 + p\frac{1}{r}\frac{\partial}{\partial r}\left[K(r)\frac{\partial w_1}{\partial r}\right] + \nabla^4 w_1 = \left(\frac{1}{r}\frac{\partial^2 w_0}{\partial r^2}\frac{\partial \Phi_0}{\partial r} + \frac{1}{r}\frac{\partial^2 \Phi_0}{\partial r^2}\frac{\partial w_0}{\partial r}\right) - 2D_0 D_1 w_0 - cD_0 w_0 + G\cos(\Omega t_0) \tag{45}$$

$$w_1 = 0, \quad \frac{\partial w_1}{\partial r} = 0 \quad \text{at} \quad r = b, 1 \tag{46}$$

The solution of Eqs. (41) and (42) has the form

$$w_0(r,t_0,t_1) = \sum_{m=1}^{\infty} \phi_{0m}(r)\left[A_m(t_1)e^{i\omega_{0m}t_0} + \bar{A}_m(t_1)e^{-i\omega_{0m}t_0}\right] \tag{47}$$

where the A_m are complex-valued functions of the slow time scale t_1, the $\bar{A}_m$ are their complex conjugates, and the $\phi_{0m}(r)$ and ω_{0m} are the axisymmetric mode shapes and natural frequencies defined by the eigenvalue problem:

$$\nabla^4 \phi_{0m} + p\frac{1}{r}\frac{d}{dr}\left[K(r)\frac{d\phi_{0m}}{dr}\right] - \omega_{0m}^2 \phi_{0m} = 0$$

$$\phi_{0m} = 0 \quad \text{and} \quad \frac{d\phi_{0m}}{dr} = 0 \quad \text{at} \quad r = b, 1 \tag{48}$$

The linear free vibration problem for the heated annular plate was solved by Arafat et al. [20] for both axisymmetric and asymmetric modes. In general, unless the temperature gradient is zero across the plate (i.e., $\tau = 1$), analytical solutions are not available. Therefore, a shooting method was used to numerically determine the natural frequencies and mode shapes, which are normalized such that $\int_b^1 r\phi_{nm}^2 dr = 1$. In Fig. 2, we show an example of the first and second axisymmetric mode shapes.

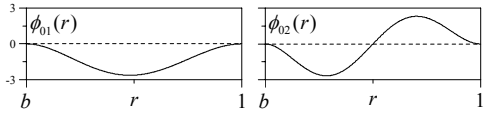

Figure 2. The first and second axisymmetric mode shapes of heated annular plate.

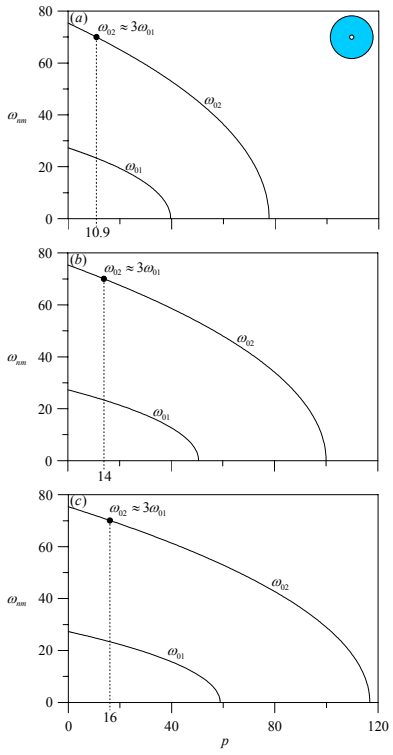

Figure 3. Variation of the first two axisymmetric natural frequencies ω_{01} and ω_{02} with p when $b = 0.1$: (a) $\tau = 2$, (b) $\tau = 1$, and (c) $\tau = 0.5$.

Among other internal resonances, Arafat et al. [20] found that, as the thermal load p is increased, a three-to-one internal resonance between the first and second axisymmetric modes is possible; that is, $\omega_{02} \approx 3\omega_{01}$. This is illustrated in Fig. 3 for a plate having $b = 0.1$ and in Fig. 4 for a plate having $b = 0.5$, where we plot variation of ω_{01} and ω_{02} with the thermal load p. In each figure, we show three cases of $\tau = 2$, $\tau = 1$, and $\tau = 0.5$.

For $\tau = 2$, the temperature at the inner boundary is greater than the temperature at the outer boundary; for $\tau = 1$, the temperatures at both boundaries are equal and there is no temperature gradient across the radius; and for $\tau = 0.5$, the temperature at the inner boundary is less than the temperature at the outer boundary. In all six cases, we find that as the thermal load p is increased, ω_{02} approaches $3\omega_{01}$. The corresponding values of $p(\equiv p_r)$, ω_{01}, and ω_{02} are presented in Table 1.

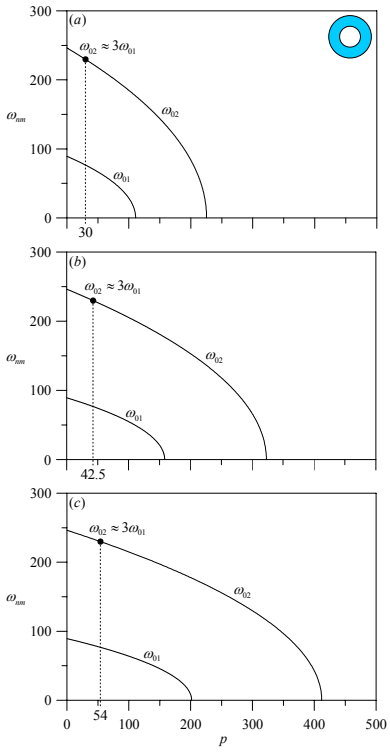

Figure 4. Variation of the first two axisymmetric natural frequencies ω_{01} and ω_{02} with p when $b = 0.5$: (a) $\tau = 2$, (b) $\tau = 1$, and (c) $\tau = 0.5$.

From this point on, as we are only considering here axisymmetric modes and for the sake of minimizing clutter, we will drop the zero from the subscript in ϕ_{0m} and ω_{0m}. Thus, to describe the internal resonance condition, we introduce the detuning parameter σ such that

$$\omega_2 = 3\omega_1 + \varepsilon\sigma \tag{49}$$

Moreover, for primary resonance of the second mode, we introduce the detuning parameter δ such that

$$\Omega = \omega_2 + \varepsilon\delta \tag{50}$$

Table 1. Values of the coefficients in the evolution equations.

	$b = 0.1$			$b = 0.5$		
	$\tau = 2$	$\tau = 1$	$\tau = 0.5$	$\tau = 2$	$\tau = 1$	$\tau = 0.5$
p_r	10.963	13.937	16.122	29.985	42.697	54.180
ω_{01}	23.323	23.345	23.362	76.580	76.610	76.636
ω_{02}	69.968	70.036	70.086	229.741	229.829	229.909
α_1	720.740	718.852	717.493	10840.408	10831.674	10823.664
α_2	−2200.116	−2193.962	−2189.732	−27787.998	−27768.494	−27753.133
α_3	−195.908	−192.442	−189.876	−1332.518	−1325.807	−1319.506
β_1	11560.882	11544.578	11535.053	152400.435	152332.814	152288.869
β_2	−2200.114	−2193.964	−2189.725	−27787.166	−27768.564	−27753.279
β_3	−65.303	−64.147	−63.292	−444.180	−441.939	−439.829
Γ/G	0.056	0.056	0.056	0.019	0.019	0.019

Because damping is present in the system, it is assumed that, after some time, the contribution from all of the modes other than those directly or indirectly excited will vanish. Therefore, the long-time response of the plate is given by

$$w_0 = \phi_1\left(A_1 e^{i\omega_1 t_0} + \bar{A}_1 e^{-i\omega_1 t_0}\right) + \phi_2\left(A_2 e^{i\omega_2 t_0} + \bar{A}_2 e^{-i\omega_2 t_0}\right) \tag{51}$$

Substituting Eq. (51) into Eq. (43) and solving the resulting problem, we obtain

$$\begin{aligned}\Phi_0 = {} & \psi_1(r)\left(A_1^2 e^{2i\omega_1 t_0} + \bar{A}_1^2 e^{-2i\omega_1 t_0} + 2A_1\bar{A}_1\right) \\ & + \psi_2(r)\left(A_2^2 e^{2i\omega_2 t_0} + \bar{A}_2^2 e^{-2i\omega_2 t_0} + 2A_2\bar{A}_2\right) \\ & + \psi_3(r)\left[A_1 A_2 e^{2i(\omega_1+\omega_2)t_0} + \bar{A}_1\bar{A}_2 e^{-2i(\omega_1+\omega_2)t_0}\right. \\ & \left. + A_1\bar{A}_2 e^{2i(\omega_1-\omega_2)t_0} + \bar{A}_1 A_2 e^{-2i(\omega_1-\omega_2)t_0}\right]\end{aligned} \tag{52}$$

where the spatial functions $\psi_i(r)$ are defined by the following boundary-value problems:

$$\left(\frac{d^2}{dr^2} + \frac{1}{r}\frac{d}{dr} - \frac{1}{r^2}\right)\psi_i' = f_i(r) \quad \text{for} \quad i = 1,2,3 \tag{53}$$

$$\left(\frac{d}{dr} - \frac{\nu}{r}\right)\psi_i' = 0 \quad \text{at} \quad r = b,1 \tag{54}$$

Here, the prime denotes differentiation with respect to r and

$$f_1(r) = -\frac{1}{2r}\phi_1'^2, \quad f_2(r) = -\frac{1}{2r}\phi_2'^2, \quad f_3(r) = -\frac{1}{r}\phi_1'\phi_2' \tag{55}$$

Since we have a third-order equation for the ψ_i with only two boundary conditions, we can only obtain a unique solution for ψ_i'. One approach is to express the solution in a series of Bessel functions of the first and second kind of order 1. This analytical approach is further explained in [4] for circular plates. However, since the mode shapes were obtained numerically [20], we

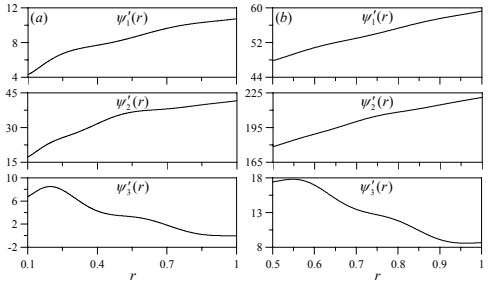

Figure 5. The spatial functions ψ_i' for $\tau = 2$ and (a) $b = 0.1$ and (b) $b = 0.5$.

choose to determine the functions $\psi_i'(r)$ numerically by a shooting method as well. As an example, we show in Fig. 5 the functions $\psi_i'(r)$ for $\tau = 2$ and (a) $b = 0.1$ and (b) $b = 0.5$.

Next, we substitute Eqs. (51) and (52) into Eq. (45), use Eqs. (49) and (50), eliminate the terms that produce secular terms [21], and obtain the equations that govern the behavior of A_1 and A_2 with t_1 as:

$$2i\omega_1\left(\frac{dA_1}{dt_1}+\mu_1 A_1\right)+\alpha_1 A_1^2\bar{A}_1=\alpha_2 A_1 A_2\bar{A}_2+\alpha_3\bar{A}_1^2 A_2 e^{i\sigma t_1} \tag{56}$$

$$2i\omega_2\left(\frac{dA_2}{dt_1}+\mu_2 A_2\right)+\beta_1 A_2^2\bar{A}_2=\beta_2 A_1\bar{A}_1 A_2+\beta_3 A_1^3 e^{-i\sigma t_1}+\Gamma e^{i\delta t_1} \tag{57}$$

where

$$\alpha_1=-3\int_b^1\phi_1\left(\phi_1'\psi_1'\right)'dr,\ \ \alpha_2=2\int_b^1\phi_1\left(\phi_1'\psi_2'+\phi_2'\psi_3'\right)'dr,$$

$$\alpha_3=\int_b^1\phi_1\left(\phi_2'\psi_1'+\phi_1'\psi_3'\right)'dr \tag{58}$$

$$\beta_1=-3\int_b^1\phi_2\left(\phi_2'\psi_2'\right)'dr,\ \ \beta_2=2\int_b^1\phi_2\left(\phi_2'\psi_1'+\phi_1'\psi_3'\right)'dr,$$

$$\beta_3=\int_b^1\phi_2\left(\phi_1'\psi_1'\right)'dr \tag{59}$$

$$\Gamma=\frac{1}{2}\int_b^1 Gr\phi_2 dr,\quad \mu_k=\frac{1}{2}\int_b^1 cr\phi_k^2 dr \tag{60}$$

The values of the coefficients in the evolution equations for $b = 0.1$ and 0.5 and $\tau = 2$, 1, and 0.5 are presented in Table 1. Using integration by parts on Eqs. (58) and (59) and making use of Eqs. (53)-(55), one can show that the α_k and β_k satisfy the symmetry conditions: $\alpha_2 = \beta_2$ and $\alpha_3 = 3\beta_3$. Such symmetries are a characteristic of systems which are conservative in the absence of damping and external forces. Therefore, one can derive the modulation equations from a time-averaged Lagrangian and a virtual work term.

Introducing the polar transformation

$$A_1(t_1)=\frac{1}{2}a_1(t_1)e^{i\left[\gamma_1(t_1)+\frac{1}{3}(\delta+\sigma)t_1\right]} \tag{61}$$

$$A_2(t_1)=\frac{1}{2}a_2(t_1)e^{i[\gamma_2(t_1)+\delta t_1]} \tag{62}$$

into Eqs. (56) and (57), we obtain the equations governing the evolution of the amplitudes and phases of vibrations as

$$a_1'=-\mu_1 a_1+\frac{\alpha_3}{8\omega_1}a_1^2 a_2\sin(\gamma_2-3\gamma_1) \tag{63}$$

$$a_1\gamma_1'=-\frac{1}{3}(\delta+\sigma)a_1+\frac{\alpha_1}{8\omega_1}a_1^3-\frac{\alpha_2}{8\omega_1}a_1a_2^2-\frac{\alpha_3}{8\omega_1}a_1^2a_2\cos(\gamma_2-3\gamma_1) \tag{64}$$

$$a_2'=-\mu_2 a_2-\frac{\beta_3}{8\omega_2}a_1^3\sin(\gamma_2-3\gamma_1)-\frac{\Gamma}{\omega_2}\sin\gamma_2 \tag{65}$$

$$a_2\gamma_2'=-\delta a_2+\frac{\beta_1}{8\omega_2}a_2^3-\frac{\beta_2}{8\omega_2}a_1^2a_2-\frac{\beta_3}{8\omega_2}a_1^3\cos(\gamma_2-3\gamma_1)-\frac{\Gamma}{\omega_2}\cos\gamma_2 \tag{66}$$

where the prime here indicates the derivative with respect to t_1.

The fixed points of the evolution equations are obtained by setting the $a_i' = 0$ and $\gamma_i' = 0$ in Eqs. (63)-(66) and then solving for the roots. The stability of the solutions is ascertained by examining the eigenvalues of the Jacobian matrix obtained from the evolution equations. There are two possible cases: (1) $a_1 = 0$ and $a_2 \equiv \hat{a}_2 \neq 0$ and (2) $a_1 \neq 0$ and $a_2 \neq 0$. The first case corresponds to single-frequency (ω_2) periodic vibrations of the plate and the second case corresponds to two-frequency (ω_1 and ω_2) periodic vibrations of the plate. In the first case, the single-mode solutions $\hat{a}_2$ can obtained in closed-form from

$$\frac{\beta_1^2}{64\omega_2^2}\hat{a}_2^6-\frac{\delta\beta_1}{4\omega_2}\hat{a}_2^4+\left(\mu_2^2+\delta^2\right)\hat{a}_2^2-\frac{\Gamma^2}{\omega_2^2}=0 \tag{67}$$

In addition, dynamic solutions of the evolution equations are possible and, depending on their nature, they correspond to either quasiperiodic or chaotic vibrations of the plate. Such solutions are calculated numerically through long-time integration and a shooting method and the stability of limit cycles is ascertained using Floquet theory [24].

In Fig. 6, we present typical force-response curves for a plate with $b = 0.1$, $\tau = 0.5$, $\sigma = 50$, and $\delta = 50$. As the forcing amplitude Γ is increased from zero, a stable single-mode solution $\hat{a}_2$ develops. This solution then loses stability through a saddle-node bifurcation, resulting in a jump to a higher-amplitude single-mode solution. Decreasing the value of Γ to a relatively small

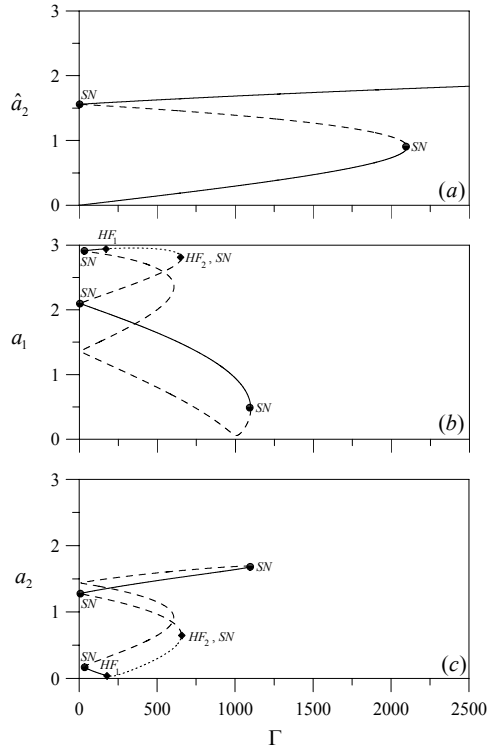

Figure 6. Force-response curves for a plate with $b = 0.1$ and $\tau = 0.5$ when $\sigma = 50$ and $\delta = 50$: $\hat{a}_2$ denotes single-mode responses and $a_1 - a_2$ denotes two-mode responses; HF_1 and HF_2 denote Hopf bifurcations and SN denotes a saddle-node bifurcation. Solid lines (——) denote stable equilibrium solutions, dashed lines (– – –) denote unstable equilibrium solutions, and dotted lines $(\cdots\cdots)$ denote unstable foci.

value (≈ 11), we find that $\hat{a}_2$ loses stability through another saddle-node bifurcation. Depending on the initial conditions, the response could jump down to the lower-amplitude $\hat{a}_2$ branch or to a coexisting two-mode $a_1 - a_2$ solution.

The two-mode equilibrium solutions are found to be isolated from $\hat{a}_2$ and do not come about as a result of a pitchfork bifurcation. For a certain range of $\Gamma \in [40, 186]$, two stable $a_1 - a_2$ branches coexist. The longer stable branch has relatively close-matching values of the amplitudes a_1 and a_2, with a_1 decreasing with increasing Γ. In contrast, the shorter stable branch has very small values of a_2 and quite large values of a_1. That is, on this branch, even though the second mode is excited near primary resonance, most of the response consists of the first mode.

Moreover, as we increase Γ past 168.4, this equilibrium solution goes through a supercritical Hopf bifurcation HF_1 and a limit cycle is born, corresponding to quasiperiodic oscillations of the plate. A projection of the limit cycle onto the $a_1 - a_2$ plane is shown in Fig. 7a soon after the bifurcation. As Γ increases, this limit cycle persists and grows in size as shown in Fig. 7b

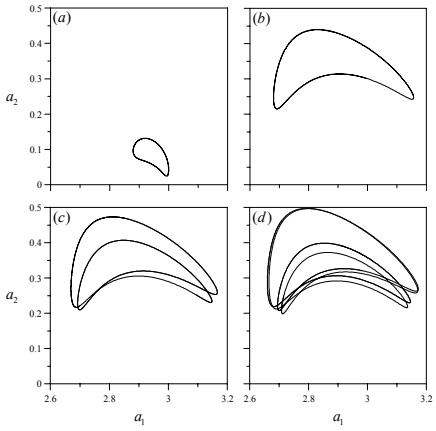

Figure 7. Two-dimensional projections of the limit cycles, born out of a supercritical Hopf bifurcation at $\Gamma_{HF_1} = 168.4$, onto the $a_1 - a_2$ plane for a plate of $b = 0.5$ and $\tau = 0.5$ when $\sigma = 50$ and $\delta = 50$: $\Gamma_a = 170$ (P1), $\gamma_b = 200$ (P1), $\Gamma_c = 202$ (P2), and $\Gamma_d = 203$ (P4).

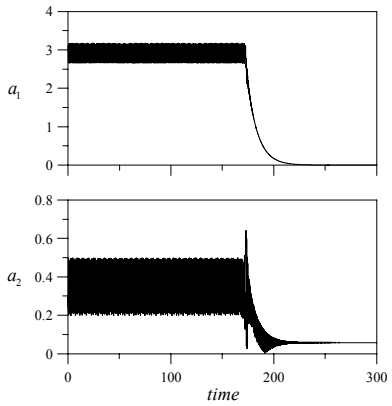

Figure 8. Time histories for a_1 and a_2 showing the period-4 limit cycle in Fig. 5d undergoing a boundary crisis and the solution tending to the stable single-mode equilibrium solution.

for $\Gamma = 200$. It then goes through a period-doubling bifurcation (Fig. 7c) and, quickly thereafter, a second period-doubling bifurcations (Fig. 7d). However, this sequence does not continue, but rather the resulting period-four limit cycle is destroyed through a boundary crisis. Depending on the initial conditions, the solution then tends to one of three co-existing stable equilibrium solutions. In Fig. 8, we present the time histories of a_1 and a_2 for the period-four limit cycle before and after the crisis. In this case, the solution tends to the lower branch of single-mode equilibrium solutions. A second supercritical Hopf bifurcation HF_2 exists near $\Gamma = 655.3$, which is also very close to a saddle-node bifurcation. However, in this case, the resulting limit cycle almost immediately disappears through a boundary crisis as Γ is

very slightly decreased from the bifurcation point.

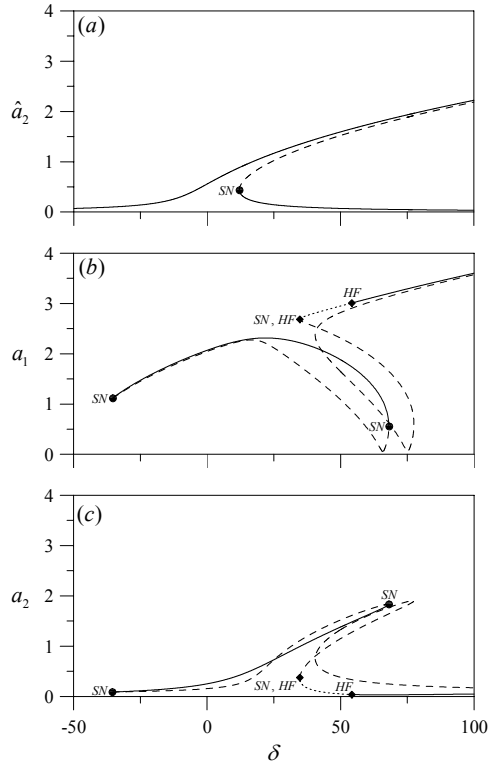

Figure 9. Frequency-response curves for a plate with $b = 0.1$ and $\tau = 0.5$ when $\sigma = 50$ and $\Gamma = 250$: $\hat{a}_2$ denotes single-mode responses and $a_1 - a_2$ denotes two-mode responses; HF_1 and HF_2 denote Hopf bifurcations and SN denotes a saddle-node bifurcation. Solid lines (——) denote stable equilibrium solutions, dashed lines (– – –) denote unstable equilibrium solutions, and dotted lines $(\cdots\cdots)$ denote unstable foci.

To explore the influence of detuning the excitation frequency on the response, we show in Fig. 9 typical frequency-response curves for the case of $b = 0.1$, $\tau = 0.5$, $\sigma = 50$, and $\Gamma = 250$. From Table 1, we note that the values of the cofficient of the effective nonlinearity for both the first and second modes (i.e., α_1 and β_1) are positive for different values of τ and b. Hence, generally, both modes exhibit a hardening-spring behavior. This is illustrated in Fig. 9a, where the single-mode response curves $\hat{a}_2$ are bent to the right, an indication of a hardening-spring behavior. In addition, in this projection of the fixed points, the two-mode solutions $a_1 - a_2$ are confined to two isolated "island" branches. The island to the left is comprised of two branches, one stable and one unstable, which connect at two saddle-node bifurcations. While on the island to the right, which extends well beyond $\delta = 100$, the stable $a_1 - a_2$ fixed points undergo Hopf bifurcations, giving rise to limit cycles (i.e., quasiperiodic oscillations of the plate).

In Fig. 10, we show the influence of detuning the internal resonance on the fixed points. From Eq. (67), it is clear that the values (but not stability) of the single-mode solution $\hat{a}_2$ are independent of the internal resonance detuning σ, which is reflected in Fig. 10a. The two-mode $a_1 - a_2$ fixed points are projected as a single island, which extends well beyond $\sigma = 100$. Once more, we find that these fixed points undergo Hopf bifurcations.

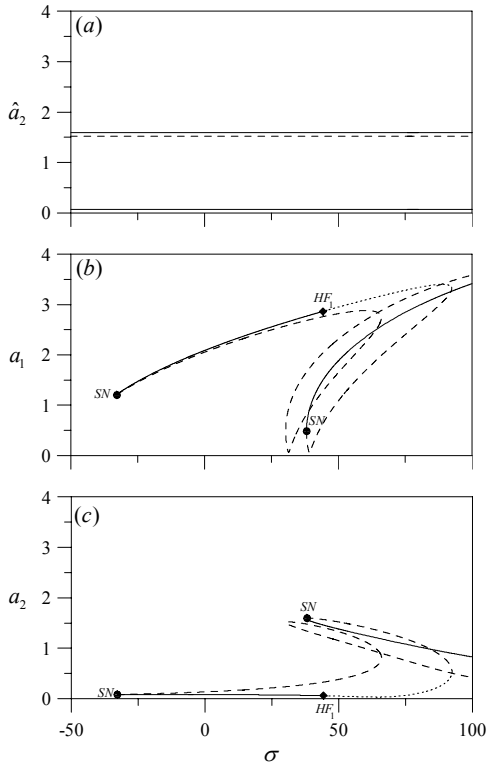

Figure 10. Frequency-response curves for a plate with $b = 0.1$ and $\tau = 0.5$ when $\delta = 50$ and $\Gamma = 250$: $\hat{a}_2$ denotes single-mode responses and $a_1 - a_2$ denotes two-mode responses; HF_1 and HF_2 denote Hopf bifurcations and SN denotes a saddle-node bifurcation. Solid lines (——) denote stable equilibrium solutions, dashed lines (– – –) denote unstable equilibrium solutions, and dotted lines $(\cdots\cdots)$ denote unstable foci.

Lastly, considering a plate with $b = 0.5$, we also found that the general character of the response curves is qualitatively similar to those in Figs. 6-10.

SUMMARY

The nonlinear responses of a thermally loaded isotropic annular plate were investigated by solving the von Kármán equa-

tions. From the linear free-vibration problem, it was found that, as the thermal load is increased, a three-to-one internal resonance between the first and second modes could occur. Therefore, we set to investigate the behavior of the plate around this internal resonance when the second mode is directly excited near primary resonance. To this end, we applied the method of multiple scales to derive the evolution equations governing the amplitudes and phases of the responses. In the process, a shooting method was used to solve for the mode shapes and spatial stress functions.

We determined equilibrium solutions of the evolution equations, corresponding to periodic oscillations of the plate, and demonstrated their behavior by way of force- and frequency-response curves. We found two types of equilibrium solutions: single-mode $\hat{a}_2$ and two-mode $a_1 - a_2$. Depending on their projection, the two-mode solutions are found to be limited to either a single or two islands; that is, they do not appear as a consequence of the single-mode solution undergoing a pitchfork bifurcation. Moreover, the two-mode solutions lose stability through Hopf bifurcations. The resulting limit cycles, which correspond to quasiperiodic oscillations of the plate, then undergo period-doubling bifurcations. However, we found that the higher-period limit cycles are destroyed through a crisis.

REFERENCES

[1] Nayfeh, A. H., 2000. *Nonlinear Interactions*. Wiley, New York.

[2] Sridhar, S., Mook, D. T., and Nayfeh, A. H., 1975. "Non-Linear Resonances in the Forced Responses of Plates, Part I: Symmetric Responses of Circular Plates". *Journal of Sound and Vibration* **41**, pp. 359-373.

[3] Sridhar, S., Mook, D. T., and Nayfeh, A. H., 1978. "Non-Linear Resonances in the Forced Responses of Plates, Part II: Asymmetric Responses of Circular Plates". *Journal of Sound and Vibration* **59**, pp. 159-170.

[4] Hadian, J. and Nayfeh, A. H., 1990. "Modal Interaction in Circular Plates". *Journal of Sound and Vibration* **142**, pp. 279-292.

[5] Lee, W. K. and Kim, C. H., 1995. "Combination Resonances of a Circular Plate with Three-Mode Interaction". *Journal of Applied Mechanics* **62**, pp. 1015-1022.

[6] Yeo, M. H. and Lee, W. K., 2001. "Responses of Nonlinear Asymmetric Forced Vibrations of a Circular Plate". In Proceedings of the Third International Symposium on Vibrations of Continuous Systems. Jackson Lake, Wyoming, July 23- 27, pp. 42-44.

[7] Tauchert, T. R., 1991. "Thermally Induced Flexure, Buckling, and Vibration of Plates". *Applied Mechanics Reviews* **44**, pp. 347-360.

[8] Thornton, E. A., 1993. "Thermal Buckling of Plates and Shells". *Applied Mechanics Reviews* **46**, pp. 485-506.

[9] Awrejcewicz, J. and Krys'ko, V. A., 2003. *Nonclassical Thermoelastic Problems in Nonlinear Dynamics of Shells*. Springer, Berlin.

[10] Fedorov, V. A., 1976. "Thermostability of Elastically Clamped Variable-Stiffness Annular Plates". *Soviet Aeronautics* **19**, pp. 105-109.

[11] Irie, T. and Yamada, G., 1978. "Thermally Induced Vibration of Circular Plate". *Bulletin of the JSME* **21**, pp. 1703-1709.

[12] Buckens, F., 1979. "Vibrations in a Thermally Stressed Thin Plate". *Journal of Thermal Stresses* **2**, pp. 367-385.

[13] Pal, M. C., 1969. "Large Deflections of Heated Circular Plates". *Acta Mechanica* **8**, pp. 82-103.

[14] Pal, M. C., 1970. "Large Amplitude Free Vibration of Circular Plates Subjected to Aerodynamic Heating". *International Journal of Solids and Structures* **6**, pp. 301-313.

[15] Pal, M. C., 1973. "Static and Dynamic Non-Linear Behaviour of Heated Orthotropic Circular Plates". *International Journal of Non-Linear Mechanics* **8**, pp. 489-504.

[16] Biswas, P. and Kapoor, P., 1985. "Non-Linear Vibrations of Circular Plates at Elevated Temperature". In Proceedings of the Fourth International Conference on Numerical Methods in Thermal Problems, Part 2. Swansea, United Kingdom, July 15- 18, pp. 1493-1501.

[17] Li, S.-R., Zhou, Y.-H., and Song, X., 2002. "Non-Linear Vibration and Thermal Buckling of an Orthotropic Annular Plate with a Centric Rigid Mass". *Journal of Sound and Vibration* **251**, pp. 141-152.

[18] Nayfeh, A. H. and Faris, W., 2002. "Thermally Induced Principal Parametric Resonance in Circular Plates". *Shock and Vibration* **9**, pp. 143-150.

[19] Nayfeh, A. H. and Faris, W., 2003. "Dynamic Behavior of Circular Structural Elements Under Thermal Loads". In Proceeding of the 44th AIAA/ASME/ASCE/AHS/ASC Structures, Structural Dynamics, and Materials Conference. Norfolk, Virginia, April 7-10, pp. 1-9. Paper number AIAA-2003-1618.

[20] Arafat, H. N., Faris, W., and Nayfeh, A. H., 2003. "Vibrations and Buckling of Annular and Circular Plates Subjected to a Thermal Load". In Proceeding of the 44th AIAA/ASME/ASCE/AHS/ASC Structures, Structural Dynamics, and Materials Conference. Norfolk, Virginia, April 7-10, pp. 1-10. Paper number AIAA-2003- 1927.

[21] Nayfeh, A. H., 1981. *Introduction to Perturbation Methods*. Wiley, New York.

[22] Hetnarski, R. B., 1987. *Thermal Stresses II*. North-Holland, Amsterdam.

[23] Boley, B. A. and Weiner, J. H., 1960. *Theory of Thermal Stresses*. Wiley, New York.

[24] Nayfeh, A. H. and Balachandran, B., 1995. *Applied Nonlinear Dynamics*. Wiley, New York.